Title

The miR-15/16 cluster is involved in the regulation of vertebrate LC-PUFA biosynthesis by targeting *pparγ* as demonstrated in rabbitfish *Siganus canaliculatus*

Authors

Junjun Sun [1,3], Cuiying Chen[1,3], Cuihong You[1, 3], Yang Liu [1], Hongyu Ma[1,3], Óscar Monroig [4], Douglas R. Tocher [5], Shuqi Wang [1,3*], Yuanyou Li [2*]

Addresses

[1] Guangdong Provincial Key Laboratory of Marine Biotechnology, Shantou University, Shantou 515063, China

[2] School of Marine Sciences, South China Agricultural University, Guangzhou 510642, China

[3] STU-UMT Joint Shellfish Research Laboratory, Shantou University, Shantou 515063, China

[4] Instituto de Acuicultura Torre de la Sal, Consejo Superior de Investigaciones Científicas (IATS-CSIC), 12595 Ribera de Cabanes, Castellón, Spain

[5] Institute of Aquaculture, Faculty of Natural Sciences, University of Stirling, Stirling FK9 4LA, Scotland, UK

***Corresponding Author**

Prof. Yuanyou Li, Ph.D. (E–mail: yyli16@scau.edu.cn; Tel: 020-87571321)

Shuqi Wang, Ph.D. (E–mail: sqw@stu.edu.cn; Tel: 0754-86500614)

Abstract

Post-transcriptional regulatory mechanisms play important roles in the regulation of long-chain ($\geq C_{20}$) polyunsaturated fatty acid (LC-PUFA) biosynthesis. Here, we address a potentially important role of the miR-15/16 cluster in the regulation of LC-PUFA biosynthesis in rabbitfish *Siganus canaliculatus*. In rabbitfish, miR-15 and miR-16 were both highly responsive to fatty acids affecting LC-PUFA biosynthesis and displayed a similar expression pattern in a range of rabbitfish tissues. A common potential binding site for miR-15 and miR-16 was predicted in the 3'UTR of peroxisome proliferator-activated receptor gamma (*pparγ*), an inhibitor of LC-PUFA biosynthesis in rabbitfish, and luciferase reporter assays revealed that *pparγ* was a potential target of miR-15/16 cluster. *In vitro* individual or co-overexpression of miR-15 and miR-16 in rabbitfish hepatocyte line (SCHL) inhibited both mRNA and protein levels of Pparγ, and increased the mRNA levels of *Δ6Δ5 fads2, Δ4 fads2* and *elovl5*, key enzymes of LC-PUFA biosynthesis. Inhibition of *pparγ* was more pronounced with co-overexpression of miR-15 and miR-16 than with individual overexpression in SCHL. Knockdown of miR-15/16 cluster gave opposite results, and increased mRNA levels of LC-PUFA biosynthesis enzymes were observed after knockdown of *pparγ*. Furthermore, miR-15/16 cluster overexpression significantly increased the contents of 22:6n-3, 20:4n-6 and total LC-PUFA in SCHL with higher 18:4n−3/18:3n−3 and 22:6n-3/22:5n-3 ratio. These suggested that miR-15 and miR-16 as a miRNA cluster together enhanced LC-PUFA biosynthesis by targeting *pparγ* in rabbitfish. This is the first report of the participation of miR-15/16 cluster in LC-PUFA biosynthesis in vertebrates.

Key words

miR-15/16 cluster· *pparγ· Δ6Δ5 fads2· Δ4 fads2·* LC-PUFA biosynthesis· Rabbitfish *Siganus canaliculatus*

1. Introduction

Long-chain ($\geq C_{20}$) polyunsaturated fatty acids (LC-PUFA) including arachidonic acid (ARA; 20:4n-6), eicosapentaenoic acid (EPA; 20:5n-3) and docosahexaenoic acid (DHA; 22:6n-3) are highly bioactive fatty acids with crucial physiological functions in humans and other animals (Janssen and Kiliaan 2014; Calder 2015). It is commonly known that fish, especially marine fish, are major dietary sources of the health promoting n-3 LC-PUFA (e.g. DHA and EPA) for human consumption (Tur et al. 2012; Nordøy and Dyerberg 2015). However, most marine fish do not possess or lack the ability to endogenously convert C_{18} PUFA such as α-linolenic acid (ALA; 18:3n-3) to $C_{20\text{-}22}$ LC-PUFA due the lower activity and/or the absence of the complete pathway for LC-PUFA biosynthesis (Tocher 2015).

The rabbitfish is an exception to the above pattern since this herbivorous marine teleost has the ability to biosynthesize LC-PUFA from C_{18} PUFA. The pathway requires a series of fatty acid desaturations and elongations catalyzed by fatty acyl desaturase (*fads*) and elongation of very-long-chain fatty acids (*elovl*) enzymes, respectively, and key enzymes required for LC-PUFA biosynthesis including *Δ6Δ5 fads2*, *Δ4 fads2*, *elovl4* and *elovl5* have been isolated and functionally characterized rabbitfish (Li et al. 2010; Monroig et al. 2012). Consequently, *S. canaliculatus* serves as a good model for studying the regulatory mechanisms of LC-PUFA biosynthesis in teleosts (Li et al. 2008). Thus, in recent years, considerable research in rabbitfish has demonstrated that *fads* and *elovl* genes were regulated by transcription factors including sterol regulatory element binding protein 1 (*srebp1*), liver X receptor (*lxr*) and hepatic nuclear factor 4

alpha (*hnf4α*), and enhanced LC-PUFA biosynthesis by increasing expression of *Δ4* and *Δ6Δ5 fads2* (Zhang et al. 2016a; Dong et al. 2016, 2018; Wang et al. 2018). In addition, the transcription factor peroxisome proliferator-activated receptor gamma (*pparγ*) negatively influenced the biosynthesis of LC-PUFA in rabbitfish by down-regulating *Δ6Δ5 fads2* expression (Li et al. 2019).

Peroxisome proliferator-activated receptors such as PPARγ belong to the steroid hormone receptor superfamily and were so named as they can be activated by peroxisome proliferators (Mangelsdorf et al. 2000). Generally, PPAR can be activated by natural or artificial ligands, then heterodimerize with retinoid X receptor (RXR), and subsequently bind to PPAR response element (PPRE) in target genes and thereby influence transcriptional regulation (Adeghate et al. 2011). In mammals, ligand-activated PPARγ can positively regulate adipocyte differentiation, induce expression of lipoprotein lipase (LPL), and promote the storage of fatty acids (Heikkinen et al. 2007). In addition, PPARγ is a key inducer of differentiation, lipogenesis, and insulin sensitivity in white and brown adipocytes and is involved in lipid deposition in many other cell types (Poulsen et al. 2012). While these data indicate that PPARγ is generally a positive regulatory factor in mammalian lipid metabolism, *pparγ* is a negative regulatory factor of LC-PUFA biosynthesis in rabbitfish (Li et al. 2019). Ppars gene have been cloned successfully from rabbitfish, and its role in the regulation of LC-PUFA synthesis has been preliminarily explored. It is speculated that *pparγ* might be involved in LC-PUFA biosynthesis by regulating the key enzymes expression through the Lxr/Srebp1 pathway *in vitro* (Zhang et al. 2016a; You et al. 2017).

97 Further unique post-transcriptional regulatory mechanisms have been
98 demonstrated in rabbitfish, with micro-RNAs, miR-17 and miR-146, found to be
99 involved in the regulation of LC-PUFA biosynthesis by directly targeting *Δ4 fads2* and
100 *elovl5*, respectively (Zhang et al. 2014; Chen et al. 2018). In addition, miR-33 and miR-
101 24 indirectly regulate LC-PUFA biosynthesis in rabbitfish through the Insig1/Srebp1
102 pathway by targeting *insig1* (Chen et al. 2019; Sun et al. 2019). Previous studies have
103 revealed that miR-15 and miR-16 are highly conserved in animals and play crucial roles
104 in apoptosis and the regulation of lipid metabolism, such as fat deposition and adipocyte
105 differentiation (Dong et al. 2014; Fu et al. 2018; Her et al. 2011). However, nothing is
106 currently known about the functions of miR-15 and miR-16 in the regulation of LC-
107 PUFA biosynthesis in any vertebrate.
108 Here, we report that miR-15 and miR-16 were highly responsive to ALA, EPA and
109 DHA, and bioinformatic analysis showed a common potential binding site for miR-15
110 and miR-16 in the 3'UTR of *pparγ* in rabbitfish, which prompted further investigation
111 into their possible roles in LC-PUFA biosynthesis. In mammals, miR-15 and miR-16
112 are generally found as a miRNA cluster (Lagos-Quintana 2001; Janaki et al. 2014),
113 which often forms a polycistron, and are co-transcribed with each other along with
114 nearby protein-coding genes (Baskerville et al. 2005). Compared with an individual
115 miRNA, the regulation mode of miRNA clusters is more complex and its function is
116 more efficient (Poy et al. 2004; Yu et al. 2006). Therefore, whether this was the case
117 with miR-15 and miR-16 in the regulation of LC-PUFA biosynthesis in rabbitfish was
118 worthy of investigation. Consequently, co-overexpression or individual overexpression

of miR-15 and miR-16 in the SCHL rabbitfish hepatic cell line were investigated to determine the potential role of the miR-15/16 cluster in the regulation of LC-PUFA biosynthesis. Furthermore, knockdown of the miR-15/16 cluster and *pparγ* were carried out for further verification. The resultant data form the basis for elucidating the mechanism of miR-15/16 cluster involvement in the regulation of LC-PUFA biosynthesis in rabbitfish, and provide us with novel insights into the mechanisms of regulation of LC-PUFA biosynthesis in vertebrates, which may contribute to the optimization and/or enhancement of the LC-PUFA pathway in teleosts.

2. Materials and Methods

2.1 Experimental animals and tissue collection

All procedures performed on fish were in accordance with the National Institutes of Health guide for the care and use of Laboratory animals (NIH Publications No. 8023, revised 1978) and approved by the Institutional Animal Care and Use Committee of Shantou University (Guangdong, China). Samples of brain, eyes, heart, kidney, stomach, intestine, spleen, gill, muscle and liver for tissue distribution were collected from six wild rabbitfish obtained from the coast near Nan Ao Marine Biology Station (NAMBS) of Shantou University, Southern China. Fish (196.08 ± 5.05 g) were fasted for 24 h and subsequently anesthetized with 0.01% 2-phenoxyethanol (Sigma-Aldrich, USA) prior to tissues being sampled. Immediately upon collection, tissue samples were frozen in liquid nitrogen and subsequently stored at −80 °C prior to analysis.

2.2 Cell culture

The rabbitfish *S. canaliculatus* hepatocyte line (SCHL) was previously established in our laboratory (Liu et al. 2017). Cells were cultured at 28 ℃ in Dulbecco's modified Eagle's medium/nutrient F12 (DMEM/F12, Gibco, Life Technologies, USA) containing 20 mM 4-(2-hydroxyethyl) piperazine-1-ethanesulphonic acid (HEPES, Sigma-Aldrich, USA), 10 % fetal bovine serum (FBS, Gibco, Life Technologies, USA), 0.5 % rainbow trout *Oncorhynchus mykiss* serum (Caisson Labs), penicillin (100 U ml^{-1}, Sigma-Aldrich, USA) and streptomycin (100 U ml^{-1}, Sigma-Aldrich, USA). Human embryonic kidney cells (HEK 293T, Chinese Type Culture Collection, Shanghai, China) were grown in High Glucose Dulbecco's Modified Eagle Medium (DMEM, Gibco, Life Technologies, USA) supplemented with 10 % FBS (Sijiqing Biological Engineering Material Company, China) and maintained at 37 ℃ with 5 % CO_2.

2.3 Molecular cloning of miR-15/16 cluster and sequence analysis in rabbitfish

In human, miR-15 and miR-16 are clustered within 0.5 kb at 13q14 (Lagos-Quintana 2001). In order to obtain sequence information of the miR-15/16 cluster, part of the miR-15/16 cluster gene was first cloned by PCR (LA Taq, Takara, Beijing, China) using primers (1516-part-F and 1516-part-R) designed in mature sequences of miR-15 (LM379588.1) and miR-16 (LM379591.1) of zebrafish. Genomic DNA (gDNA) prepared from rabbitfish liver (DNeasy® blood & tissue kit, Qiagen, Hilden, Germany) was used as PCR template. By alignment with rabbitfish genome sequence (BGI, Shenzhen, China), a 530 bp coincident sequence between the obtained gene sequence

and the genome sequence was found. According to the genome sequence, 1058 bp upstream (1516-ups-F and 1516-ups-R) and 978 bp downstream sequences (1516-down-F and 1516-down-R) were obtained. The secondary structure of miR-15 and miR-16 was determined by RNAfold online (http://rna.tbi.univie.ac.at/). Phylogenetic trees were constructed on the basis of nucleotide sequence alignments between rabbitfish sca-pre-miR-15 or sca-pre-miR-16 and their orthologs using the Neighbour Joining method with MEGA 6.0.

2.4 RNA isolation and quantitative real-time PCR (qPCR)

Total RNA was extracted using Trizol reagent (Invitrogen, Carlsbad, CA, USA), and concentration and quality of total RNA confirmed by spectrophotometer (NanoDrop 2000, Thermo Scientific, USA). cDNA was synthesized from 1 μg total RNA using the miScript II RT Kit (Qiagen, Hilden, Germany). The expression of miR-15 and miR-16 were determined by quantitative PCR (qPCR) using the miScript SYBR Green PCR Kit (Qiagen, Hilden, Germany) with miR-15 and miR-16 specific primers (qPCR-miR-15, qPCR-miR-16) and universal primer. For qPCR measurement of *pparγ* (JF502072.1), *Δ6Δ5 fads2* (EF424276.2), *Δ4 fads2* (GU594278.1) and *elovl5* (GU597350.1) mRNA expression levels, LightCycler® 480 SYBR Green I Master (Roche, Germany) was used with rabbitfish gene-specific primers (Table 1). The relative mRNA levels of each sample was normalized to 18s rRNA (AB276993) and calculated by the comparative threshold cycle method (Livak and Schmittgen 2012). All reactions were run in LightCycler® 480 thermocycler (Roche, Germany) using

qPCR programs according to the manufacturer's specifications.

2.5 Plasmid construction

For construction of dual luciferase reporter vectors, DNA fragments were inserted into pmirGLO dual-luciferase miRNA target expression vector (Promega, Madison, WI, USA) by digestion with *Sac*I and *Xba*I. The recombinant vectors were: i) pmirGLO-*pparγ*-3'UTR; A partial DNA fragment including the binding site of miR-15 and miR-16 in rabbitfish *pparγ* 3'UTR was amplified by *pparγ*-3'UTR-F/R primers and then inserted into pmirGLO vector; ii) pmirGLO-*pparγ*-3'UTR-MU; A 43 nt oligonucleotide of the *pparγ* 3'UTR containing a mutated binding site for miR-15 and miR-16 was synthesized (Sangon Biotech, Shanghai, China) using mutation primers named *pparγ*-3'UTR-Mu-F/R, such that the predicted binding site of miR-15 and miR-16 in the *pparγ* 3'UTR 5'-TGCTGCT-3' was mutated to 5'-GGTTACG-3' to prevent complementarity of miR-15/16 and then annealed and ligated into the pmirGLO vector. The PCR reactions were performed using high-fidelity *pfu* DNA polymerase (Tiangen Biotech, Beijing, China) and the insert fragments of recombinant plasmids were sequenced (Sangon Biotech).

2.6 Rabbitfish SCHL cells incubation with PUFA

Polyunsaturated fatty acid (Cayman Chemical Co., Ann Arbor, USA) / bovine serum albumin (BSA, fatty acid free, Cayman, USA) complexes of ALA, EPA and DHA at 10 mM concentration were prepared according to Ou et al. (2001) and stored at

−20 °C. SCHL cells were seeded into six-well plates at a density of 5×10^5 cells per well in DMEM/F12 supplemented with 5 % FBS and 0.2 % rainbow trout serum. After 24 h, cells were incubated for 1 h in serum-free DMEM/F12 prior to incubation with 100 μM ALA-BSA, EPA-BSA or DHA-BSA complexes in triplicate wells in serum-free medium. Each assay was incubated with equal amounts of BSA. After 24 h incubation, cells were lysed and harvested for total RNA extraction.

2.7 Transfection of SCHL cells with miRNA mimic or inhibitor

miRNA mimics or inhibitors were transfected into SCHL cells to achieve up-regulation or down-regulation of miRNA expression, respectively. The miRNA mimics (dsRNA oligonucleotides), miRNA inhibitors (single-stranded oligonucleotides) and NC oligonucleotides (negative control) were obtained from Genepharma (Shanghai, China). SCHL cells were seeded into 6-well plates or 100 mm vessels, grown for 24 h to 80 % confluence in DMEM/F12 supplemented with 10 % FBS and 0.5 % rainbow trout serum, and triplicate wells transfected with 50 or 150 nM of each oligonucleotide using Lipofectamine® 2000 Reagent according to the manufacturer's instructions (Invitrogen, Carlsbad, CA, USA). After transfection for 24 h or 48 h, cells were harvested for qPCR analysis and Western blotting.

2.8 Dual-luciferase experiment to confirm the interaction between miR-15/16 and *pparγ*

To determine whether *pparγ* was a direct target gene of miR-15 and miR-16, a dual

luciferase assay was performed using human embryonic kidney cells (HEK 293T; Chinese Type Culture Collection, Shanghai, China) seeded in 96-well cell culture plates. Cells were grown for 24 h to 80 % confluence and then co-transfected with either miRNA mimics (50 nM) or NC (50 nM) with different recombinant dual luciferase reporter vectors (50 ng) using Lipofectamine™ 2000 Transfection Reagent (Invitrogen). Firefly and Renilla luciferase activities were quantified after 48 h transfection using a microplate reader (Infinite M200 Pro, Tecan, Switzerland) with firefly luciferase activity normalized to Renilla luciferase activity. Eight replicate wells were used for each treatment.

2.9 Western blotting

For miR-15/16 cluster target identification at the protein level, Western blotting was used to detect the protein expression level of Pparγ. Total protein was extracted at 48 h post-transfection using cell total protein extraction kit (Sangon Biotech) and concentrations quantified with non-interference protein assay kit (Sangon Biotech). Aliquots of protein (20~40μg) were loaded and separated on a 10 % sodium dodecyl sulphate-polyacrylamide gel (SDS/PAGE), transferred onto polyvinylidene fluoride (PVDF) membranes (Millipore, USA) with a semidry transfer cell (Bio-Rad Trans Blot SD, USA). After incubating in blocking buffer (Tris-Buffered Saline Tween (TBST) containing 5% dried skimmed milk powder) for 2 h at room temperature, membranes were incubated at 4 ℃ overnight with rabbit polyclonal antibody against human PPARγ (1:500; predicted molecular weight: ~54 kDa) (Wanleibio, Shenyang, China), and

mouse monoclonal antibody against β-actin (1:2000; ~42 kDa) (Immunoway, USA). After three washes with TBST, membranes were incubated with HRP goat anti-rabbit/mouse IgG (Abcam, USA) secondary antibodies at a ratio of 1:5000. Membranes were washed three times with TBST, and immunoreactive bands were visualized using the Amersham Imager 600 (GE Healthcare, USA) and the intensity of each band analyzed with Image J software (version 1.8.0, NIH, Bethesda, MD, USA). The optical density of each sample was normalized by β-actin for statistical analysis, and three independent experiments were conducted.

2.10 RNA interference

Silencing of *pparγ* expression was performed using small interfering RNA (siRNA) duplexes (Genepharma, Shanghai, China) with the following sequences: si-*pparγ* sense, 5'-CCUCCCAAACAGUCAGAUUdTdT-3'; si-*pparγ* antisense, 5'-AAUCUGACUGUUUGGGAGGdTdT-3'. The SCHL cells were seeded into 6-well plates, grown for 24 h to 80 % confluence and subsequently transfected with 50 nM of *pparγ*-specific siRNA (siRNA-*pparγ*) or negative control using Lipofectamine® 2000 Reagent. The cells were harvested for qPCR analysis at 24 h post-transfection.

2.11 Fatty acids isolation and GC analysis

SCHL cells were seeded into100 mm plates at a density of 2×10^6 cells per plate or six-well plates at a density of 5×10^5 cells per well, grown for 24 h to 80 % confluence, and triplicate wells transfected with 150 or 50 nM miRNA mimics or NC using

Lipofectamine® 2000 Reagent (Invitrogen, Carlsbad, CA, USA). After 48 h post-transfection, SCHL cells were harvested for qPCR and fatty acid composition analysis. Fatty acid composition of cell total lipid was analyzed by gas chromatography (GC) after chloroform/methanol extraction, saponification and methylation with boron trifluoride (Sigma-Aldrich, USA) as described previously (Li et al. 2010; Chen et al. 2016). For identification, the retention times of the fatty acid methyl esters were compared to those of standards (Sigma-Aldrich, USA), with quantification of each fatty acid in a certain number of cells (10^7 cells) being estimated using the signal of the internal standard C21:0 (heptadecanoic acid) (Sigma-Aldrich). Fatty acid contents were expressed as a percentage of total fatty acids (Table 2).

2.12 Statistical analysis

All data were presented as means ± SEM with n value as stated. Significance of differences among groups were analyzed by one-way analysis of variance (ANOVA) followed by Tukey's multiple comparison test or Student's t-test at a significance level of $P < 0.05$ using SPSS 19.0 software (SPSS Inc, Chicago, IL).

3. Results

3.1 The sequence, structure and tissue distribution of rabbitfish miR-15 and miR-16

Based on rabbitfish genomic data, the gene sequence of the miR-15/16 cluster was cloned, and mature miR-15 and miR-16 encoding capability was found to be clustered

within 0.5 kb (Fig. 1). In rabbitfish, miR-16 is located upstream of miR-15 (Fig. 1), which was consistent with that of human (Lagos-Quintana 2001). Through multiple alignment with its orthologs in other species, the precursor and mature sequences of miR-15 and miR-16 were identified, and a 7 nt common "seed sequence" (AGCAGCA), which is pivotal for target recognition of miRNA, was identified at the 5′ end of the rabbitfish miR-15 and miR-16 (Supplementary Fig. S1 and S2). The rabbitfish sca-pre-miR-15 (58 nt) and sca-pre-miR-16 (80 nt) contained the typical stable stem-loop secondary structure necessary for mature miRNA processing (Supplementary Fig. S3). Phylogenetic analysis showed that sca-pre-miR-15 and sca-pre-miR-16 clustered together with those of other fish species and have close homologous relationships with zebrafish and Atlantic salmon (Fig. 2).

To determine whether miR-15 and miR-16 co-transcribed with each other in rabbitfish, the abundance of miR-15 and miR-16 mRNA were determined in selected tissues. The results showed that miR-15 and miR-16 were widely expressed in the examined tissues with highest expression level in brain, and intermediate levels in stomach, intestine, gill, kidney, spleen, eye and heart, and low expression in muscle and liver (Fig. 3).

3.2 miR-15 and miR-16 show similar responses to PUFA in rabbitfish SCHL cells *in vitro*

In order to study the role of the miR-15/16 cluster in LC-PUFA biosynthesis, SCHL cells were incubated with 100μM ALA, EPA and DHA. *In vitro*, the expression levels

of both miR-15 and miR-16 were higher in SCHL cells supplemented with ALA, with the expression of miR-15 significantly higher compared to BSA controls (Fig. 4a). The expression levels of both miR-15 and miR-16 were lower in SCHL cells supplemented with EPA or DHA, with the expression of miR-16 significantly lower compared to BSA controls (Fig. 4b and 4c).

3.3 Rabbitfish *pparγ* is a target of miR-15 and miR-16

Bioinformatic analysis showed that potential binding sites of miR-15 and miR-16 were present in the 3'UTR of *pparγ* in rabbitfish (Fig. 5a). Based on this finding, dual luciferase assays were used to verify the interaction between the miR-15/16 cluster and *pparγ*. Results from the qPCR analysis revealed that HEK 293T cells transfected with miR-15 and miR-16 mimics had levels of rabbitfish miR-15 and miR-16 expression 16-fold and 11-fold higher than NC, respectively ($P < 0.01$) (Fig. 5b). If the heterologous expression of miRNA interacts with the inserted target fragment, the luciferase activity will be reduced. As shown in Fig. 5c, heterologous expression of miR-15, miR-16 and miR-15/16 mimics effectively reduced luciferase activities when co-transfected with pmirGLO-*pparγ*-3'UTR reporter plasmid into HEK 293T cells (Fig. 5c, lanes 5-8). In particular, the luciferase activity was lowest with co-transfection of the miR-15/16 mimic (Fig. 5c, lane 8). However, when mutation was introduced into the predicted miR-15 and miR-16 binding sites in the 3′UTR of *pparγ* mRNA, the inhibition was eliminated (Fig. 5c, lanes 9-12). Additionally, the Pparγ protein levels in SCHL cells transfected with miR-15 mimic, miR-16 mimic and miR-15/16 mimic were lower than

that of cells transfected with NC (Fig. 6). In particular, the inhibition effect of miR-15/16 mimic on Pparγ protein expression was stronger than that of individual miR-15 mimic and miR-16 mimic. In summary, these data demonstrate that *pparγ* may be a common target gene of miR-15 and miR-16.

3.4 miR-15/16 cluster up-regulates expression of *Δ6Δ5 fads, Δ4 fads* and *elovl5* by targeting *pparγ* in rabbitfish hepatocytes

The potential role of the miR-15/16 cluster in the regulation of LC-PUFA biosynthesis was further investigated by overexpression and knockdown of miR-15/16 cluster. The qPCR analysis showed that the expression of target gene *pparγ* was reduced, whereas the expression levels of genes of key enzymes involved in LC-PUFA synthesis, i.e. *Δ6Δ5 fads2*, *elovl5*, *Δ4 fads2*, were increased by overexpression of the miR-15/16 cluster in SCHL cells (Fig. 7a). In contrast, the expression levels of *Δ6Δ5 fads2*, *elovl5* and *Δ4 fads2* mRNAs were significantly reduced, and the expression of *pparγ* increased, by miR-15/16 cluster knockdown in SCHL cells (Fig. 7b). In consequence, miR-15/16 cluster can promote LC-PUFA biosynthesis in rabbitfish hepatocytes.

To investigate whether the miR-15/16 cluster was involved in LC-PUFA biosynthesis by targeting *pparγ*, the expression of *pparγ* was silenced by RNA interference technology. After silencing, the expression of *pparγ* was reduced significantly, whereas the expression levels of key enzyme genes involved in LC-PUFA synthesis, i.e. *Δ6Δ5 fads2*, *elovl5* and *Δ4 fads2*, were increased with the expression of *Δ6Δ5 fads2*, and *Δ4 fads2* being significantly higher (Fig. 8).

3.5 Up-regulation of the miR-15/16 cluster promoted biosynthesis of LC-PUFA in rabbitfish hepatocytes

Whether decreasing the endogenous level of *pparγ* by overexpression of miR-15/16 cluster affected LC-PUFA biosynthesis was assessed in SCHL cells *in vitro*. Co-overexpression or individual overexpression of miR-15 and miR-16 in SCHL cells resulted in 16-fold and 13-fold higher levels of miR-15 in cells receiving miR-15 mimic and miR-15/16 mimic, respectively, as well as 11-fold and 8-fold higher levels of miR-16 in cells receiving miR-16 mimic and miR-15/16 mimic, respectively ($P < 0.01$), at 48 h post transfection compared to NC (Fig. 9a). In addition to lower levels of *pparγ* mRNA by overexpression of miR-15/16 cluster in SCHL cells (Fig. 9b). Fatty acid analysis showed that miR-15 overexpression resulted in higher conversion of ALA to C18:4n−3 and C22:5n-3 to DHA. Overexpression of miR-16 and co-overexpression of miR-15/16 cluster both resulted in higher conversion of ALA to C18:4n−3, EPA to C22:5n-3 and C22:5n-3 to DHA (Fig. 9b). Compared with the NC group, the contents of DHA and ARA, products of LC-PUFA biosynthesis, and total LC-PUFA accumulation in SCHL cells increased either by co-overexpression or individual overexpression of miR-15 and miR-16, and among them, the accumulation level of LC-PUFA was highest with co-overexpression of miR-15 and miR-16 (Table 2).

4. Discussion

Post-transcriptional regulatory mechanisms have been shown to play important

roles in the regulation of LC-PUFA biosynthesis in rabbitfish (Zhang et al. 2014, 2016b; Chen et al. 2018, 2019; Sun et al. 2019). However, the mechanisms of post-transcriptional regulation of LC-PUFA biosynthesis by miRNAs remains largely unclear, and nothing is known on the regulation of LC-PUFA biosynthesis by miRNA clusters. Here, we investigated a potentially important role of miR-15/16 cluster in the regulation of LC-PUFA biosynthesis in rabbitfish.

Previous studies have revealed that miR-15 and miR-16 are highly conserved in animals and play crucial roles in the regulation of lipid metabolism including fat deposition and adipocyte differentiation (Dong et al. 2014; Fu et al. 2018; Her et al. 2011). In humans, miR-15 and miR-16 belong to a common precursor family and are highly conserved, and clustered within 0.5 kb at 13q14 (Lagos-Quintana 2001). In the present study, we cloned the sequence of the miR-15/16 cluster in rabbitfish, and found that miR-15 and miR-16 were clustered on the same chromosome within 0.5 kb. Multiple alignment with its orthologs in other species showed the mature sequences of miR-15 (22 nt) and miR-16 (23 nt) are highly conserved in rabbitfish. Generally, miRNAs depend on the "seed sequence" to identify and partially combine with the 3'UTR of target genes, thereby inducing target mRNA degradation or inhibiting protein translation. The seed sequences of rabbitfish miR-15 and miR-16 showed high identity to those of other species, which suggested that miR-15 and miR-16 may perform similar functions in rabbitfish. In addition, miRNA clusters often form a polycistron, and co-transcribe with each other along with nearby protein-coding genes in mammals (Baskerville et al. 2005). In the present study, miR-15 and miR-16 displayed a similar

405 expression pattern in different rabbitfish tissues, as well as in hepatocytes incubated
406 with different PUFA that influence LC-PUFA biosynthesis. These above evidences
407 indicated that miR-15 and miR-16 as a miRNA cluster may be co-transcribed with each
408 other and have a combined effect on LC-PUFA biosynthesis in rabbitfish.

409 To further understand how the miR-15/16 cluster was involved in the regulation of
410 LC-PUFA biosynthesis in rabbitfish, bioinformatic analysis showed that common
411 potential binding sites of miR-15 and miR-16 were predicted in the 3'UTR of *pparγ*,
412 which is the transcription factor that plays a role in the negative regulation of LC-PUFA
413 biosynthesis in rabbitfish (Li et al. 2019). Dual luciferase assays revealed that *pparγ*
414 may be a direct target gene of miR-15 and miR-16. *In vitro*, overexpression of miR-15
415 and miR-16 significantly decreased both the mRNA and protein abundance of Pparγ in
416 SCHL, but suggested that the negative regulation of miR-15 and miR-16 predominantly
417 occurred at the translational level since the effect on protein level was greater than on
418 mRNA level. It was demonstrated previously that, compared with an individual miRNA,
419 regulation by miRNA clusters was more complex and functionally more efficient (Poy
420 et al. 2004; Yu et al. 2006). A similar situation was also found in rabbitfish as the
421 decrease of Pparγ expression in SCHL cells was more significant with co-
422 overexpression of miR-15 and miR-16 than that with overexpression of miR-15 or miR-
423 16 individually, suggesting that *pparγ* may be a common direct target gene of both miR-
424 15 and miR-16. Moreover, co-overexpression or individual overexpression of miR-15
425 and miR-16 in SCHL cells increased the mRNA levels of *Δ6Δ5 fads2, Δ4 fads2* and
426 *elovl5*. Consistent with this, inhibition of miR-15 and/or miR-16 resulted in the opposite

effect, decreased expression of *Δ6Δ5 fads2, Δ4 fads2* and *elovl5*. However, individual overexpression of miR-15 or miR-16 had a stronger regulatory effect on the mRNA levels of the LC-PUFA biosynthesis enzymes than that of co-overexpression of miR-15 and miR-16. Elovl and Fad enzymes are considered as the key enzymes for the biosynthesis of LC-PUFA and the enzymes activities will ultimately affect the LC-PUFA biosynthetic capability (Tocher et al. 2003). Previous studies demonstrated that Elovl and Fad enzymes were regulated by multiple transcriptional factors in vertebrates, such as Srebp1, Hnf4α, Lxrα and Pparγ, and negative feedback mechanisms may be present in the overexpression system (Chen et al. 2019; Sun et al. 2019; Zhang et al. 2016a). This may be one reason why the effect on expression of these key enzyme genes was lower in cells co-transfected with both miR-15 and miR-16 than in cells transfected with miR-15 or miR-16 individually. In SCHL, PPAR agonists 2-bromopalmitate (2-Bro) and fenofibrate (FF) increased the expression of *pparγ*, and induced the expression changes of *Δ6Δ5 fads2, Δ4 fads2* and *elovl5*, which indicated that *pparγ* might be involved in LC-PUFA biosynthesis by regulating the key enzymes expression in rabbitfish (You et al. 2017). In the present study, silencing the expression of *pparγ* and along with that the levels of *Δ6Δ5 fads2, Δ4 fads2* and *elovl5* mRNAs were significantly increased. Based on the above data, we therefore speculated that miR-15 and miR-16 may participate together in the regulation of LC-PUFA biosynthesis in rabbitfish by targeting *pparγ*.

In order to investigate the potential role of the miR-15/16 cluster in the regulation of LC-PUFA biosynthesis in rabbitfish, we investigated whether decreasing *pparγ* by

449 overexpression of miR-15/16 affected LC-PUFA biosynthesis in SCHL cells. As stated
450 above, down-regulation of *pparγ* by miR-15 and miR-16 overexpression increased the
451 contents of DHA and ARA, products of LC-PUFA biosynthesis, and also total LC-
452 PUFA accumulation in SCHL cells. In rabbitfish, functional characterization showed
453 that Δ6/Δ5 Fads2 could efficiently convert 18:3n-3 and 18:2n-6 to 18:4n-3 and 18:3n-
454 6, respectively (Li et al. 2010). Here, we observed that overexpression of miR-15 and
455 miR-16 caused an increase in 18:4n−3/18:3n−3, which indicates an increase in Δ6Δ5
456 Fads2 enzymatic activity. This was consistent with the results of our previous study in
457 which knock-down of *pparγ* in SCHL increased conversion of 18:3n−3 to 18:4n−3 and
458 18:2n−6 to 18:3n−6, while overexpression of *pparγ* led to lower conversions, and
459 ultimately to significantly lower ARA, EPA and DHA production (Li et al. 2019). In
460 some basal vertebrate lineages, such as teleosts, the production of DHA from EPA can
461 occur directly via a Δ4 desaturase that produces DHA from the EPA elongation product,
462 22:5n-3 (Li et al. 2010; Castro et al. 2016). We showed that overexpression of miR-15
463 and miR-16 caused an increase in ratio of 22:6n-3/22:5n-3 in rabbitfish hepatocyte cells,
464 which indicates an increase in Δ4 Fads2 enzymatic activity. These were consistent with
465 the above results of mRNA expression in SCHL. However, individual overexpression
466 of miR-15 or miR-16 had a stronger regulatory effect on the conversion ratio levels of
467 the LC-PUFA biosynthesis enzymes than that of co-overexpression of miR-15 and miR-
468 16. In the above discussion, it has been mentioned that Elovl and Fad enzymes were
469 regulated by multiple transcriptional factors in vertebrates, such as Srebp1, Hnf4α, Lxrα
470 and Pparγ, and negative feedback mechanisms may be present in the overexpression

system, which might led to the above results (Chen et al. 2019; Sun et al. 2019; Zhang et al. 2016a). As expected, co-overexpression of miR-15 and miR-16 resulted in the highest accumulation of LC-PUFA, which suggested that there might be cooperativity among the miR-15/16 cluster to promote LC-PUFA biosynthesis in rabbitfish. Taken together, these results suggested that the miR-15/16 cluster could promote LC-PUFA biosynthesis by negatively regulating *pparγ* activation, and subsequently, promoted the expression of *pparγ* target genes required for LC-PUFA biosynthesis.

In summary, we confirmed that miR-15 and miR-16 are present in a miRNA cluster and together enhanced LC-PUFA biosynthesis by targeting *pparγ* in rabbitfish. To our knowledge, this is the first report of the cooperativity between miR-15 and miR-16 in the regulation of LC-PUFA biosynthesis in a vertebrate. How exactly miR-15 and miR-16 are co-transcribed and combine to function together requires further investigation.

Acknowledgements

This work was financially supported by the National Key R&D Program of China (2018YFD0900400), National Natural Science Foundation of China (No. 31873040 & No. 31702357), Natural Science Foundation of Guangdong Province (2018A030313910), China Agriculture Research System (CARS-47), Innovation and Strong School Projects in Guangdong Province (2016KTSCX037) and STU Scientific Research Foundation for Talents (NTF19019).

Compliance with Ethical Standards

Conflict of Interest The authors declare that they have no conflict of interest.

References

Adeghate E, Adem A, Hasan MY, Tekes K, Kalasz H (2011) Suppl 2: medicinal chemistry and actions of dual and pan ppar modulators. The Open Medicinal Chemistry Journal 5(2): 93-98.

Baskerville S, Bartel DP (2005) Microarray profiling of microRNAs reveals frequent coexpression with neighboring miRNAs and host genes. RNA 11(3): 241-247.

Calder PC (2015) Very long chain omega-3 (n-3) fatty acids and human health. Eur J Lipid Sci Tech 116(10): 1280-1300.

Castro LF, Tocher DR, Monroig Ó (2016) Long-chain polyunsaturated fatty acid biosynthesis in chordates: insights into the evolution of fads and elovl gene repertoire. Prog Lipid Res 62(6): 25-40.

Chen CY, Sun BL, Guan WT, Bi YZ, Li PY, Ma J, Chen F, Pan Q, Xie QM (2016) N-3 essential fatty acids in Nile tilapia, *Oreochromis niloticus*: effects of linolenic acid on non-specific immunity and anti-inflammatory responses in juvenile fish. Aquaculture 450: 250-257.

Chen CY, Wang SQ, Zhang M, Chen BJ, You CH, Xie DZ, Liu Y, Zhang QH, Zhang JY, Monroig Ó, Tocher DR, Waiho K, Li YY (2019) miR-24 is involved in vertebrate LC-PUFA biosynthesis as demonstrated in marine teleost *siganus canaliculatus*. BBA-Mol Cell Biol L 1864(5): 619.

Chen CY, Zhang JY, Zhang M, You CH, Liu Y, Wang SQ, Li YY (2018) miR-146a is involved in the regulation of vertebrate LC-PUFA biosynthesis by targeting elovl5 as demonstrated in rabbitfish *siganus canaliculatus*. Gene S0378111918309260-. DOI: 10.1016/j.gene.2018.08.063.

Dong PY, Mai Y, Zhang ZY, Mi L,Wu GF, Chu GY, Yang GS, Sun SD (2014) miR-15a/b promote adipogenesis in porcine pre-adipocyte via repressing foxo1. Acta Biochim Biophys Sin 46(7): 565-571.

Dong YW, Wang SQ, Chen JL, Zhang QH, Liu Y, You CH, Monroig Ó, Tocher DR, Li YY (2016) Hepatocyte Nuclear Factor 4α (HNF4α) Is a Transcription Factor of

522 Vertebrate Fatty Acyl Desaturase Gene as Identified in Marine Teleost *Siganus*
523 *canaliculatus*. Plos One 11: e0160361.
524 Dong YW, Zhao JH, Chen JL, Wang SQ, Liu Y, Zhang QH, You CH, Monroig Ó, Tocher
525 DR, Li YY (2018) Cloning and characterization of Δ6/Δ5 fatty acyl desaturase (fad)
526 gene promoter in the marine teleost *Siganus canaliculatus*. Gene 647: 174-180.
527 Fu SY, Yan FB, Chen YD, Sun GR, Li ZJ, Han RL, Kang XT, Li GX (2018) The
528 Function of miR-15a in regulating intramuscular fat deposition in pectoralis muscle
529 in chicken． Animal. Husbandry. Veterinary. Medicine 50(4): 60-65．
530 Her GM, Hsu CC, Hong JR, Lai CY, Hsu MC, Pang HW, Chan SK, Pai WY (2011)
531 Overexpression of gankyrin induces liver steatosis in zebrafish (*danio rerio*). BBA-
532 Mol Cell Biol L 1811(9): 536-548.
533 Heikkinen S, Auwerx J, Argmann CA (2007) PPAR gamma in human and mouse
534 physiology. Biochim Biophys Acta 1771(8): 999-1013.
535 Janaki Ramaiah M, Lavanya A, Honarpisheh M, Zarea M, Bhadra U, Bhadra MP (2014)
536 miR-15/16 complex targets p70s6 kinase1 and controls cell proliferation in mda-
537 mb-231 breast cancer cells. Gene 552(2): 255-264.
538 Janssen CI, Kiliaan AJ (2014) Long-chain polyunsaturated fatty acids (LC-PUFA) from
539 genesis to senescence: the influence of LC-PUFA on neural development, aging,
540 and neurodegeneration. Prog Lipid Res 53 (53): 1-17.
541 Lagos-Quintana M, Rauhut R, Lendeckel W (2001) Identification of novel genes
542 coding for small expressed RNAs. Science 294(5543): 853-858.
543 Livak KJ, Schmittgen TD (2012) Analysis of Relative Gene Expression Data Using
544 Real-Time Quantitative PCR and the $2^{-\Delta\Delta CT}$ Method. Methods 25: 402-408.
545 Li YY, Monroig Ó, Zhang L, Wang SQ, Zheng XZ, Dick JR, You CH, Tocher DR (2010)
546 Vertebrate fatty acyl desaturase with Δ4 activity. P Natl Acad Sci USA 107(39):
547 16840-16845.
548 Li YY, Hu CB, Zheng YJ, Xia XA, Xu WJ, Wang SQ, Chen WZ, Sun ZW, Huang JH
549 (2008) The effects of dietary fatty acids on liver fatty acid composition and Δ 6 -
550 desaturase expression differ with ambient salinities in *Siganus canaliculatus*.
551 Comp Biochem Phys B 151(2): 183-190.

552 Li YY, Yin ZY, Dong YW, Wang SQ, Tocher DR, You CH (2019) Pparγ is involved in
553 the transcriptional regulation of liver LC-PUFA biosynthesis by targeting the Δ6Δ5
554 fatty acyl desaturase gene in the marine teleost *siganus canaliculatus*. Marine
555 Biotechnology 21(1): 19-29.
556 Liu Y, Zhang QH, Dong YW, You CH, Wang SQ, Li YQ, Li YY (2017) Establishment
557 of a hepatocyte line for studying biosynthesis of long-chain polyunsaturated fatty
558 acids from a marine teleost, the white-spotted spinefoot *Siganus canaliculatus*. J
559 Fish Biol 91(2): 603-616.
560 Mangelsdorf DJ, Thummel C, Beato M, Herrlich P, Schütz G, Umesono K, Blumberg
561 B, Kastner P, Mark M, Chambon P, Evans RM (2000) The nuclear receptor
562 superfamily: the second decade. Cell 83(6): 835-839.
563 Monroig Ó, Wang SQ, Zhang L, You CH, Tocher DR, Li YY (2012) Elongation of long-
564 chain fatty acids in rabbitfish *siganus canaliculatus*: cloning, functional
565 characterisation and tissue distribution of elovl5- and elovl4-like elongases.
566 Aquaculture 350: 63-70.
567 Nordøy A, Dyerberg J (2015) N−3 fatty acids in health and disease. J Intern Med 225:
568 1-3.
569 Ou J, Tu H, Shan B, Luk A, Deboseboyd RA, Bashmakov Y, Goldstein JL, Brown MS
570 (2001) Unsaturated fatty acids inhibit transcription of the sterol regulatory element-
571 binding protein-1c (SREBP-1c) gene by antagonizing ligand-dependent activation
572 of the LXR. :Proc Natl Acad Sci U S A 98: 6027-6032.
573 Poy MN, Eliasson L, Krutzfeldt J, Kuwajima J, Ma XS, Macdonald PE, Pfeffer S,
574 Tuschl T, Rajewsky N, Rorsman P, Stoffel M (2004) A pancreatic islet-specific
575 microRNA regulates insulin secretion. Nature 432(7014): 226-230.
576 Poulsen LLC, Siersbæk M, Mandrup S (2012) Ppars: fatty acid sensors controlling
577 metabolism. Semin Cell Dev Biol 23: 631-639.
578 Sun JJ, Zheng LG, Chen CY, Zhang JY, You CH, Zhang QH, Ma HY, Monroig Ó,
579 Tocher DR, Wang SQ, Li YY (2019) MicroRNAs involved in the regulation of LC-
580 PUFA biosynthesis in teleosts: miR-33 enhances LC-PUFA biosynthesis in *Siganus*
581 *canaliculatus* by targeting insig1 which in turn up-regulates srebp1. Marine

582 biotechnology 21(4):475-487.
583 Tocher DR (2015) Omega-3 long-chain polyunsaturated fatty acids and aquaculture in
584 perspective. Aquaculture 449: 94-107.
585 Tocher DR, Bell JG, Dick JR, Crampton VO (2003) Effects of dietary vegetable oil on
586 atlantic salmon hepatocyte fatty acid desaturation and liver fatty acid compositions.
587 Lipids 38(7): 723-732
588 Tur JA, Bibiloni MM, Sureda A, Pons A (2012) Dietary sources of omega 3 fatty acids:
589 public health risks and benefits. Br J Nutr 107(2): S23.
590 Wang SQ, Chen JL, Jiang DL, Zhang QH, You CH, Tocher DR, Monroig Ó, Dong YW,
591 Li YY (2018) Hnf4α is involved in the regulation of vertebrate LC-PUFA
592 biosynthesis: insights into the regulatory role of Hnf4α on expression of liver fatty
593 acyl desaturases in the marine teleost *Siganus canaliculatus*. Fish Physiol Biochem
594 44: 1-11.
595 You CH, Jiang DL, Zhang QH, Xie DZ, Wang SQ, Dong YW, Li YY (2017) Cloning
596 and expression characterization of peroxisome proliferator-activated receptors
597 (PPARs) with their agonists, dietary lipids, and ambient salinity in rabbitfish
598 *Siganus canaliculatus*. Comp Biochem Phys B 206: 54-64.
599 Yu J, Wang F, Yang GH, Wang FL, Ma YN, Du ZW, Zhang ZW (2006) Human
600 microRNA clusters: genomic organization and expression profile in leukemia cell
601 lines. Biochem Biophys Res Commun 349(1): 59-68.
602 Zhang QH, Xie DZ, Wang SQ, You CH, Monroig Ó, Tocher DR, Li YY (2014) miR-17
603 is involved in the regulation of LC-PUFA biosynthesis in vertebrates: effects on
604 liver expression of a fatty acyl desaturase in the marine teleost *Siganus*
605 *canaliculatus*. BBA-Mol Cell Biol L 1841(7): 934-943.
606 Zhang QH, You CH, Liu F, Zhu WD, Wang SQ, Xie DZ, Monroig Ó, Tocher DR, Li
607 YY (2016a) Cloning and characterization of lxr and srebp1, and their potential roles
608 in regulation of LC-PUFA biosynthesis in rabbitfish *siganus canaliculatus*. Lipids
609 51(9): 1051-1063.
610 Zhang QH, You CH, Wang SQ, Dong YW, Monroig Ó, Tocher DR, Li YY (2016b) The
611 miR-33 gene is identified in a marine teleost: a potential role in regulation of LC-

612 PUFA biosynthesis in *Siganus canaliculatus*. Sci Rep 6: 32909.

613

Table 1 Primers or oligonucleotides used for gene clone, qPCR or vector reconstruction

Aim	Gene/Vector name	Primers/Oligonucleotides	Nucleotide sequence
miR-15/16 cluster gene clone	partial sequence	1516-part-F	TAGCAGCACGTAAATATTGGAG
		1516-part-R	CACAAACCATTCTGTGCTGCTA
	upstream sequence	1516-ups-F	AAATACGTTCACACTGGGCA
		1516-ups-R	GGGTAGGAATCTGGTCCTTCTA
	downstream sequence	1516-down-F	CTTCCTTTCTCTGCCCTCATC
		1516-down-R	GTTTCAGGACTCGCTTCTATGT
Construction of reporter vectors	pmirGLO-pparγ-3'UTR	pparγ-3'UTR-F	CCCGGGTCTAGAAGGTGGACATGTGCTTACATC
		pparγ-3'UTR-R	CCCGGGGAGCTCCTGTCTGGCTACTTTCTTTATTCATC
	pmirGLO-pparγ-3'UTR-MU	pparγ-3'UTR-MU-F	CCCGGGTCTAGACTTGTGAAATTTGACAAGAAAAAGGTTACGC
		pparγ-3'UTR-MU-R	CCCGGGGAGCTCCTGTCTGGCTACTTTCTTTATTCATC
Q-PCR	miR-15	qPCR-miR-15	TAGCAGCACAGAAUGGTTTGTG
	miR-16	qPCR-miR-16	TAGCAGCACGTAAATATTGGAG
	Δ6Δ5 fads2	Δ6Δ5fads2-F	TCACTGGAACCTGCCCACAT
		Δ6Δ5fads2-R	TTCATTCTCAGACAGTGCAAACAG
	elovl5	elovl5-F	GCACTCACCGTTGTGTATCT
		elovl5-R	GCAGAGCCAAGCTCATAGAA
	pparγ	pparγ -F	CTGCTGGCTGAGTTCTCGTCT
		pparγ-R	ATGACAAAAGGCGCGTTATCTC
	18S	18S-F	CGCCGAGAAGACGATCAAAC
		18S-R	TGATCCTTCCGCAGGTTCAC

Notes: The underscore indicates the restriction site in primers

618 **Table 2** Fatty acid composition in rabbitfish hepatocytes transfected with miR-15/16 mimic and
619 negative control (NC) (μg /10^7 cells)

620

Fatty acids composition	Treatments			
	NC	miR-15 mimic	miR-16 mimic	miR-15/16 mimic
C14:0	1.46±0.16	1.78±0.20	1.22±0.17	1.93±0.30
C16:0	27.57±2.91	35.19±5.92	29.46±7.29	35.16±5.77
C18:0	15.06±1.65	18.94±3.22	17.28±2.74	19.98±2.61
C18:1n-9	17.48±1.76^{a}	18.92±1.68^{ab}	22.23±0.12^{b}	20.51±1.19^{ab}
C18:2n-6	3.45±0.29	3.77±0.39	3.37±0.30	4.16±0.39
C18:3n-6	0.72±0.07	0.54±0.12	0.44±0.08	0.63±0.09
C18:3n-3	0.60±0.07^{a}	0.43±0.08^{ab}	0.30±0.03^{b}	0.46±0.09^{ab}
C18:4n-3	1.59±0.37	1.27±0.29	1.00±0.04	1.47±0.21
C20:2n-6	1.02±0.18^{a}	0.62±0.14^{ab}	0.47±0.04^{b}	0.63±0.15^{ab}
C20:3n-6	1.28±0.09	1.23±0.10	1.32±0.08	1.37±0.09
C20:4n-6(ARA)	5.99±0.40	6.52±0.65	7.20±0.16	7.11±0.39
C20:3n-3	0.58±0.10	0.35±0.03	0.29±0.01	0.58±0.17
C20:5n-3（EPA）	4.93±0.68^{ab}	5.82±0.56^{a}	3.69±0.32^{b}	4.14±0.45^{ab}
C22:5n-3	1.49±0.27	1.53±0.35	1.72±0.37	1.66±0.36
C22:6n-3(DHA)	9.91±1.09^{a}	10.70±0.97^{ab}	13.52±0.20^{b}	13.27±0.83^{b}
∑SFA	44.10±4.59	55.92±9.18	47.95±10.62	57.07±8.50
∑MUFA	17.48±1.76^{a}	18.92±1.68^{ab}	22.23±0.12^{b}	20.51±1.19^{ab}
∑LC-PUFA	24.89±1.29	27.19±1.39	29.02±0.85	29.62±0.99
C18:4n-3/C18:3n-3	2.61±0.48	2.90±0.24	3.45±0.42	3.26±0.21
C22:5n-3/C20:5n-3	0.32±0.09	0.28±0.07	0.45±0.10	0.38±0.08
C22:6n-3/C22:5n-3	6.90±0.93	7.53±1.36	8.93±1.51	10.40±1.57

621 Notes: Data are means ± SEM (n = 3). Different superscript letters within a row represent significant
622 differences ($P < 0.05$; t-test). SFA, saturated fatty acids; MUFA, monounsaturated fatty acid; LC-
623 PUFA, long-chain polyunsaturated fatty acid

624

Figures

Fig. 1

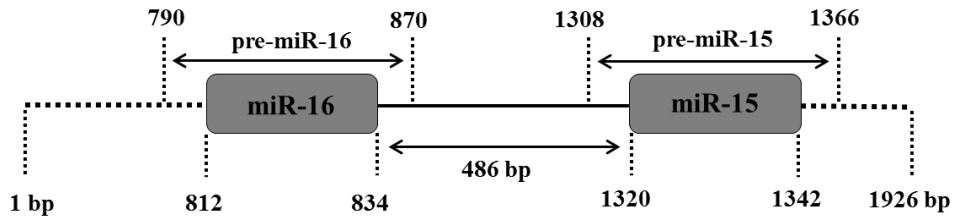

Fig. 1 The genomic structure of the rabbitfish miR-15/16 cluster. A 1926 bp gene fragment encompassing the miR-15/16 cluster was obtained. The two mature miRNAs of miR-15/16 cluster are predicted (gray boxes). Sequences between mature miRNAs including non-coding regions are indicated by black lines and the nucleotide sequence at both ends are indicated by broken line. The sequence encoding pre-miR-15 and pre-miR-16 have been noted by horizontal arrows. The vertical dotted lines with numbers indicate the positions of each element at the 1926 bp gene fragment

635 **Fig. 2**

636 **(a)**

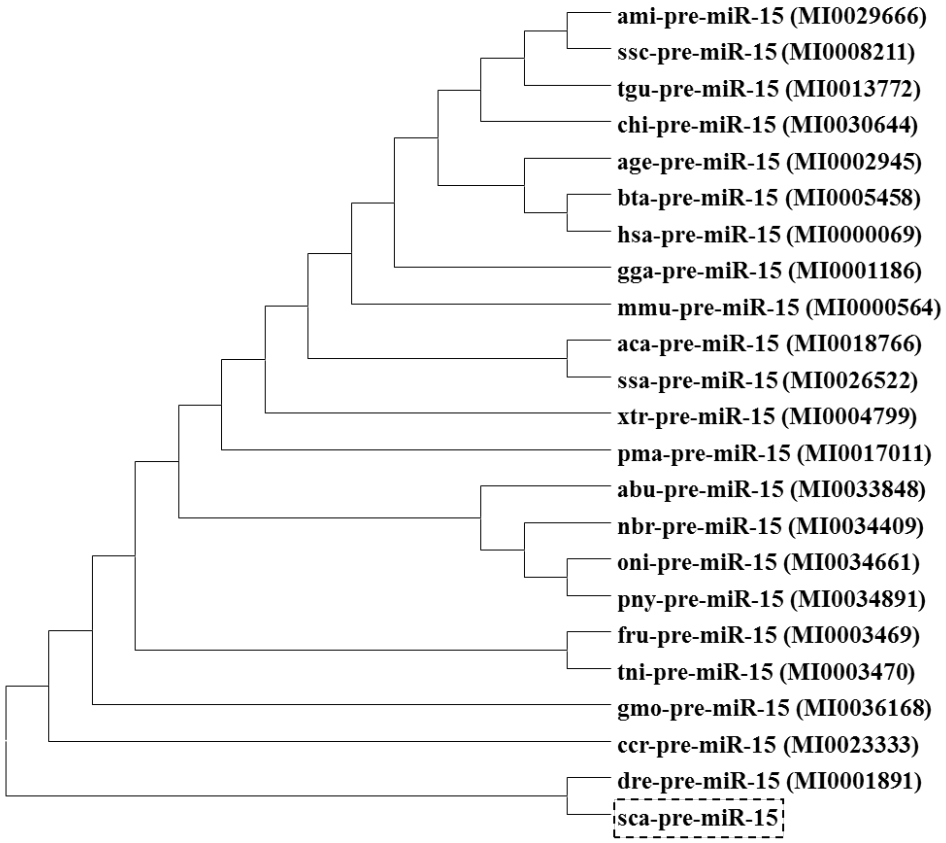

637

638 **(b)**

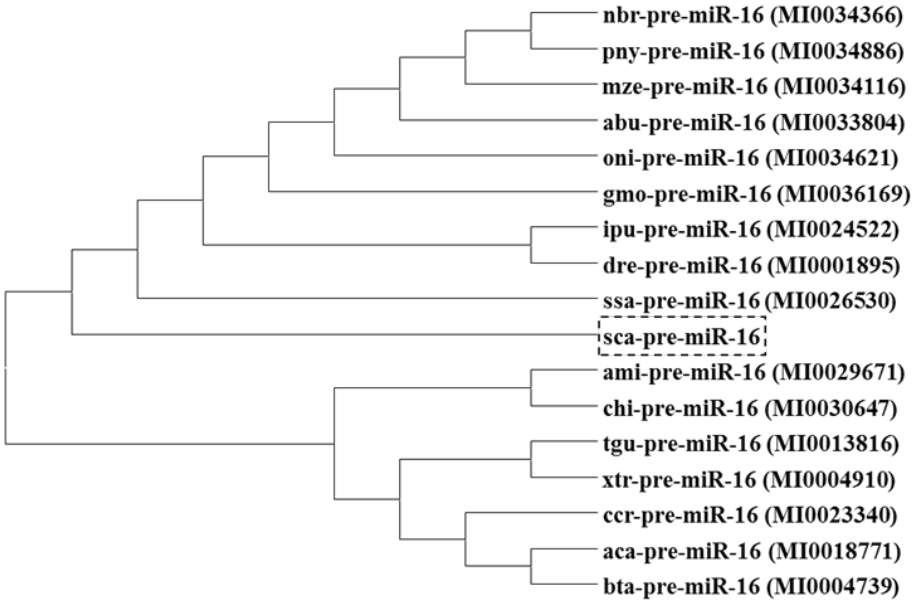

639

640 **Fig. 2** Phylogenetic trees were constructed to compare the putative rabbitfish pre-miR-15 (sca-pre-
641 miR-15) (a) and pre-miR-16 (sca-pre-miR-16) (b) nucleotide sequences with their orthologs in
642 American alligator (*Alligator mississippiensis*, ami), Wild boar (*Sus scrofa*, ssc), Zebra finch

(*Taeniopygia guttata*, tgu), Goat (*Capra hircus*, chi), Ateles geoffroy (Ateles geoffroyi, age), Cattle (*Bos taurus*, bta), Human (*Homo sapiens*, has), Junglefowl (*Gallus gallus*, gga), Mouse (*Mus musculus,* mmu), Green lizard (*Anolis carolinensis*, aca), Xenopus laevis (*Xenopus tropicalis*, xtr), Lamprey (*Petromyzon marinus*, pma), Green angel wood (*Astatotilapia burtoni*, abu), Neolamprologus bricharde (*Neolamprologus brichardi*, nbr), Tilapia (*Oreochromis niloticus*, oni), Cichlidae (*Pundamilia nyererei*, pny), Spotted green pufferfish (*Tetraodon nigroviridis*, tni) Atlantic salmon (*Salmo salar*, ssa), Carp (*Cyprinus carpio*, ccr), Takifugu rubripes (Fugu rubripes, fru), Atlantic cod (*Gadus morhua*, gmo), Channel Catfish (*Ictalurus punctatus*, ipu), Zebrafish (*Danio rerio*, dre), Metriaclima zebra (*Metriaclima zebra*, mze). miRBase accession number is in parentheses

Fig. 3

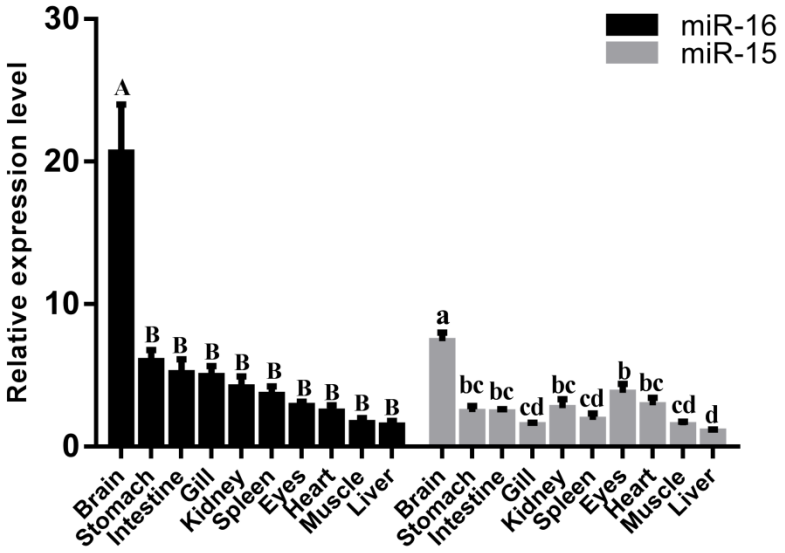

Fig. 3 Relative tissue distribution profile of miR-15 and miR-16 in rabbitfish determined by qPCR. Values are means ± SEM (n = 6) as fold change from the brain. Bars not sharing a common superscript letter indicates significant differences among the analysed tissues ($P < 0.05$; ANOVA, Tukey's test)

Fig. 4

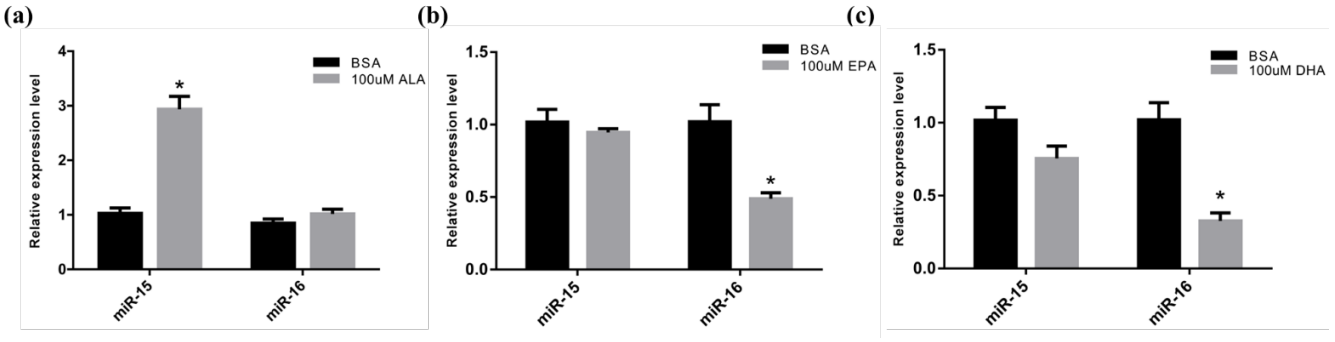

Fig. 4 Expression of miR-15 and miR-16 in SCHL cells treated with PUFA. Rabbitfish SCHL cells were incubated with ALA(a), EPA(b) and DHA(c) at 100 μM, or 0.1 % BSA (control) for 24 h, the relative levels of miR-15 and miR-16 mRNA were assessed by qPCR. Results were presented as the fold change from control in means ± SEM from three independent experiments performed in triplicate. *$P < 0.05$, student t-test

Fig. 5

(a)

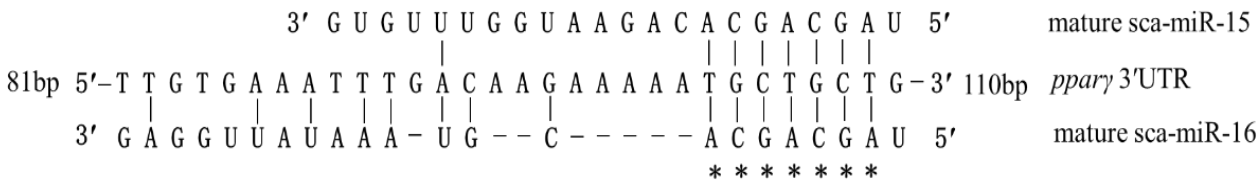

(b)

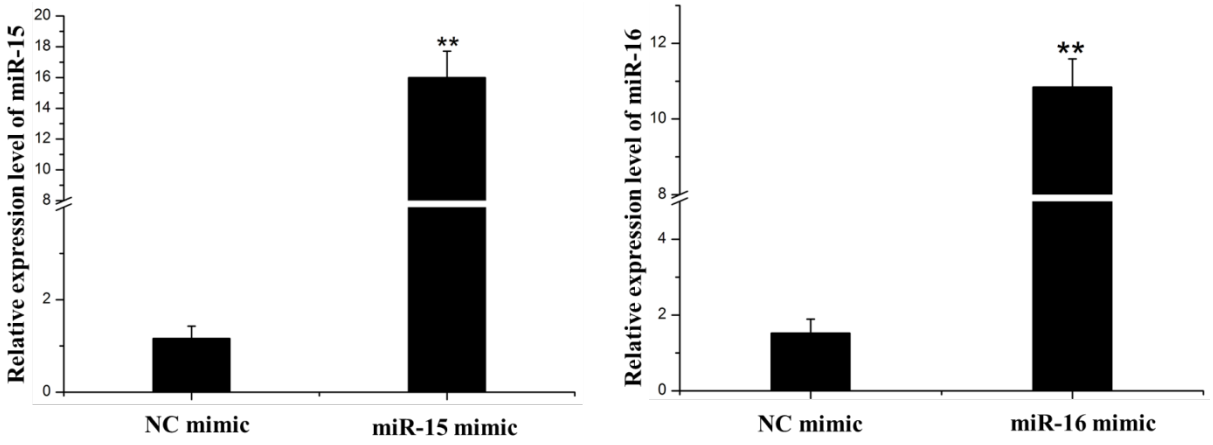

(c)

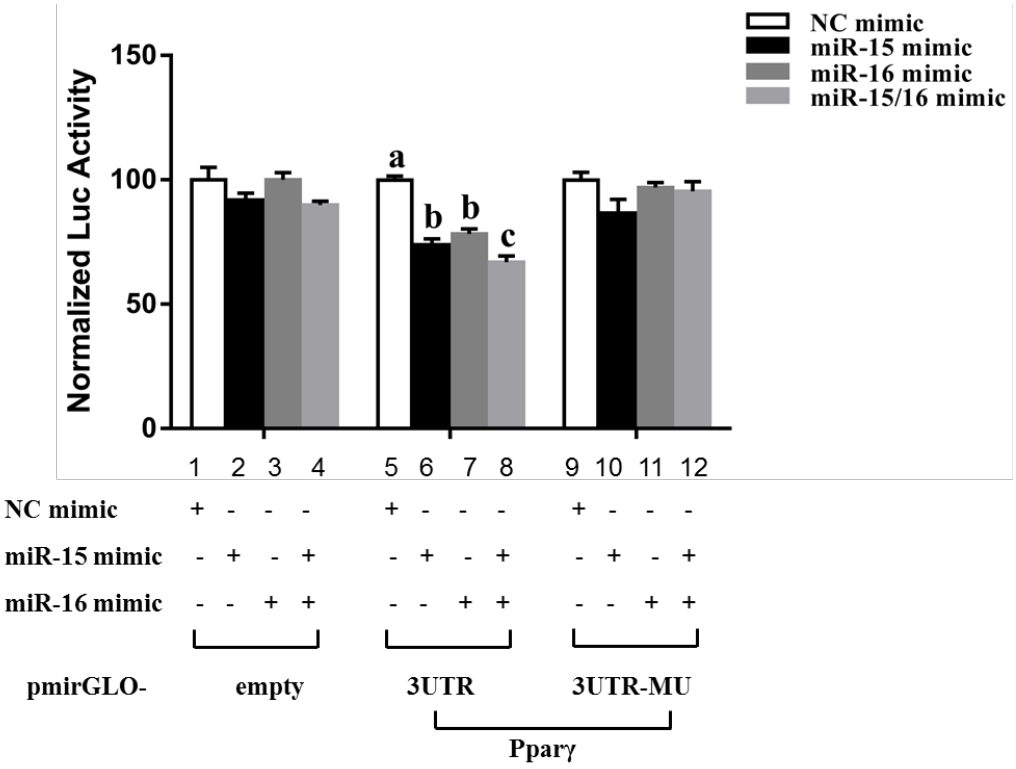

Fig. 5 miR-15/16 cluster target the 3′UTR of *pparγ*. (a) Scheme of miR-15 and miR-16 base pairing

680 the 3’UTR of the rabbitfish *pparγ*. (b) Rabbitfish miR-15 and miR-16 is over-expressed in HEK
681 293T cells by transfecting with miRNA mimics. (c) Luciferase activity in HEK 293T cells co-
682 transfected with miRNA mimic or miRNA-NC with different recombinant dual luciferase reporter
683 vectors: pmirGLO-empty as negative control (lanes 1-4); pmirGLO- PPARγ-3UTR containing
684 3′UTR of *pparγ* (lanes 5-8); pmirGLO- PPARγ -3UTR-MU with 4 nt site-directed mutation in
685 3′UTR of *pparγ* (lanes 9-12). The Renilla luciferase activity was used to normalize that of firefly
686 luciferase. Data are shown as means ± SEM (n = 8) and different superscript letters represent
687 significant differences ($P < 0.05$; ANOVA, Tukey's test)
688

689 **Fig. 6**

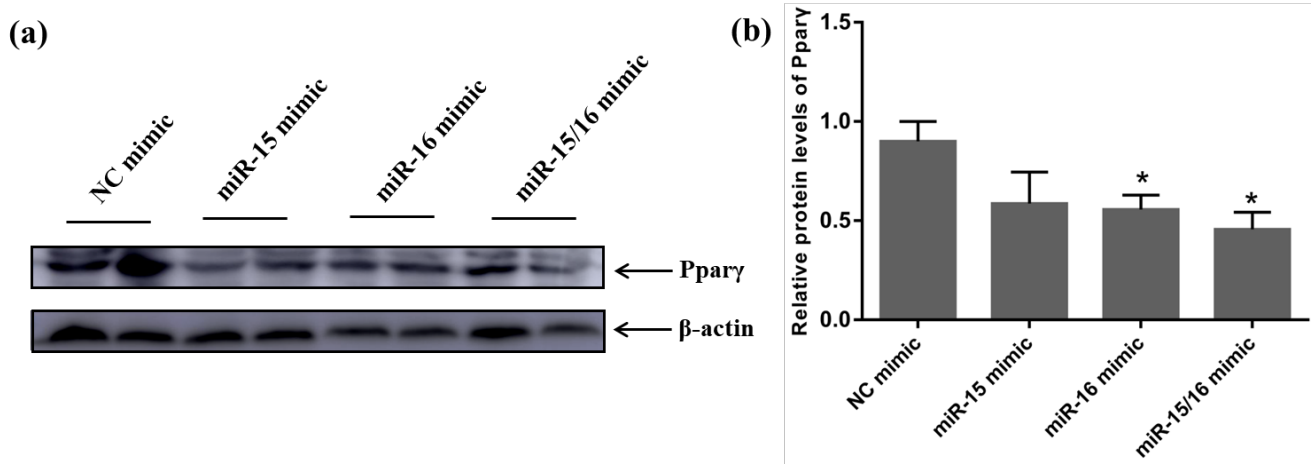

690

691 **Fig. 6** miR-15/16 cluster decrease the abundance of Pparγ at protein level. (a) Rabbitfish SCHL
692 cells were transfected with miR-15/16 mimic or NC mimic. After 48 h, aliquots of protein from cells
693 were subjected to 10% SDS-PAGE gels and immunoblot analysis of the protein levels of Pparγ (~54
694 kDa) as above. (b) The relative protein levels of Pparγ, the Image J software v1.8.0 was used to
695 quantify the intensity of the Western blotting bands. Data are means ± SEM of triplicate treatments
696 as fold change from the control (* $P < 0.05$, ** $P < 0.01$)

697

698

699 **Fig. 7**

700 **(a)**

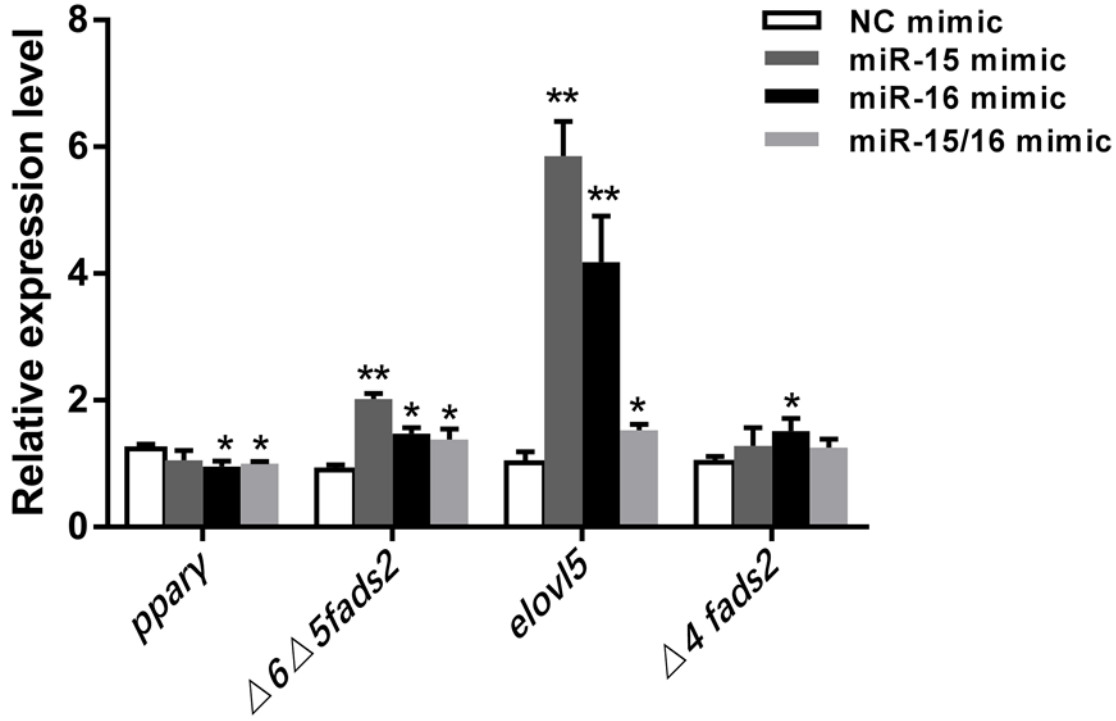

701

702 **(b)**

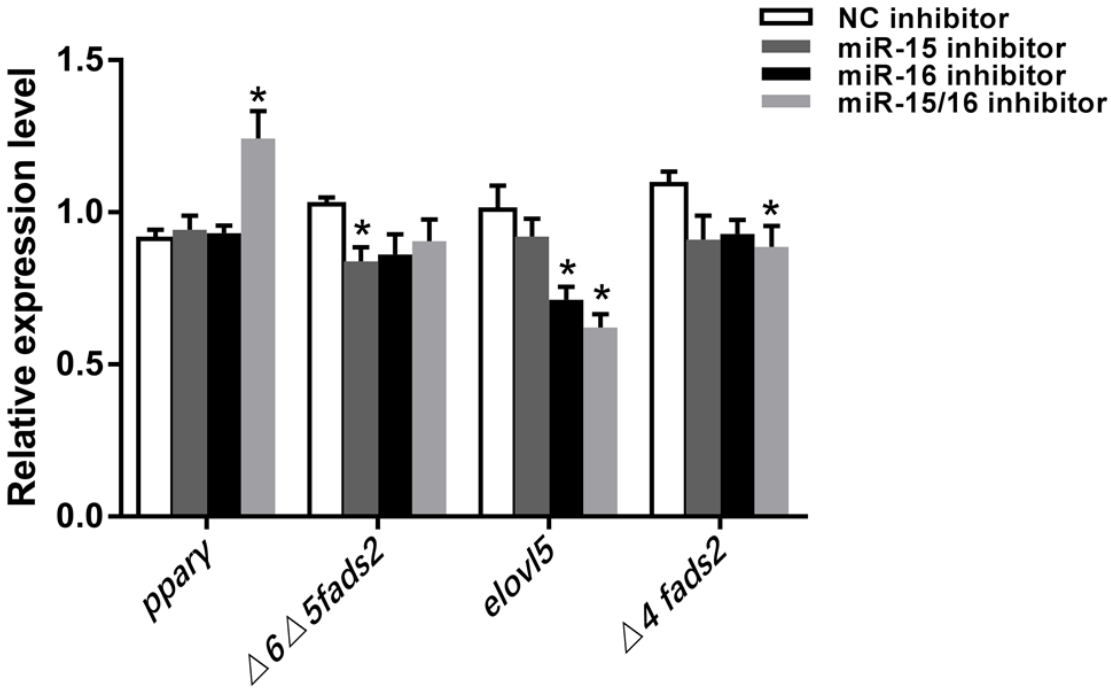

703

704 **Fig. 7** The promotion role of miR-15/16 cluster on LC-PUFA biosynthesis is mediated by *pparγ*. (a)

705 Effects of miR-15 and miR-16 overexpression on the mRNA level of *pparγ*, *Δ6Δ5 fads2*, *elovl5* and

706 *Δ4 fads2* in SCHL cells. (b) Effects of miR-15 and miR-16 inhibition on the mRNA level of *pparγ*,
707 *Δ6Δ5 fads2*, *elovl5* and *Δ4 fads2* in SCHL cells. Data are means ± SEM (n = 6). Asterisks represent
708 significant differences (* $P < 0.05$, ** $P < 0.01$; ANOVA, Tukey's test)
709
710

711 **Fig. 8**

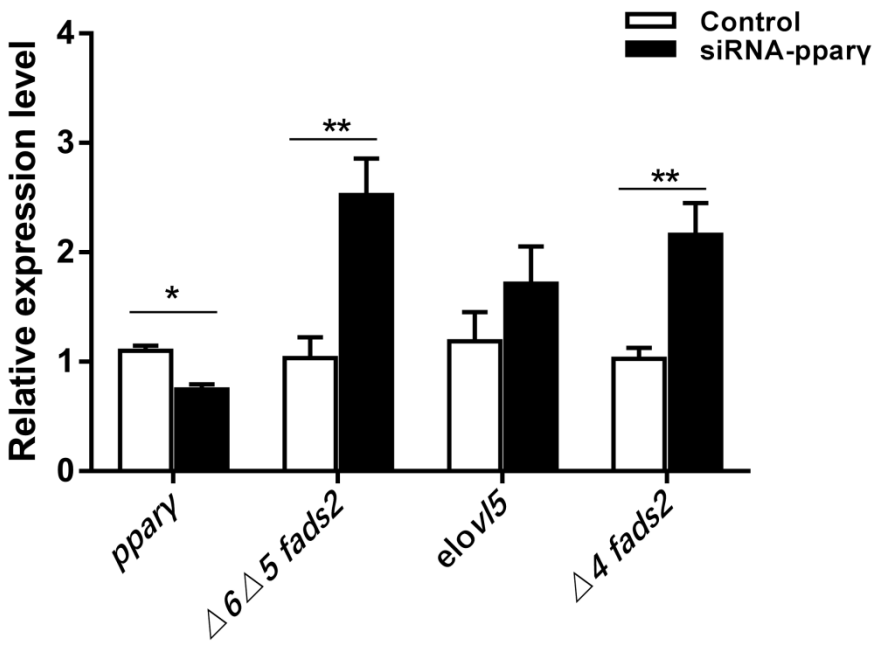

712

713 **Fig. 8** Effects of *pparγ* inhibition on the mRNA level of *pparγ*, *Δ6Δ5 fads2*, *elovl5* and*Δ4 fads2* in

714 SCHL cells. Data are means ± SEM (n = 6). Asterisks represent significant differences (* $P < 0.05$,

715 ** $P < 0.01$; ANOVA, Tukey's test)

716

Fig. 9

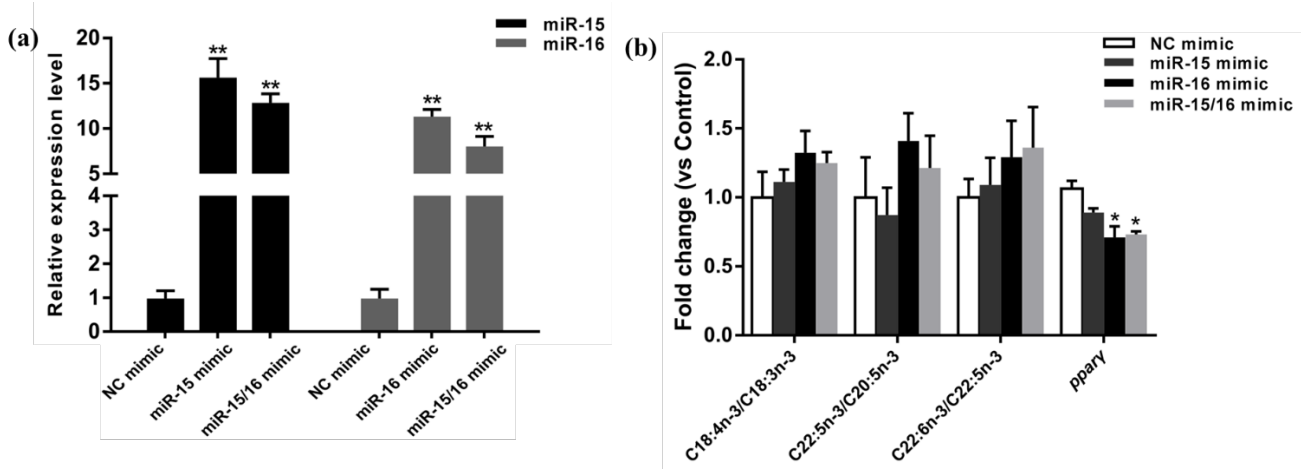

Fig. 9 Up-regulation of miR-15/16 cluster promoting LC-PUFA biosynthesis through inhibiting *pparγ* in rabbitfish hepatocytes. (a) The expression of miR-15 and miR-16 mRNA was determined by qPCR as described above. (b) The evaluation of Δ6Δ5 Fads2, Elovl5 and Δ4 Fads2 activity by desaturation and elongation indexes were performed in miR-15/16 cluster overexpressed cells and the control cells. Additionally, the expression of *pparγ* was also analyzed by qPCR as described above. Data are means ± SEM (n = 6). Asterisks represent significant differences (* $P < 0.05$, ** $P < 0.01$; ANOVA, Tukey's test)